AFM Functional Imaging on Vascular Endothelial Cells

Lilia A Chtcheglova, Linda Wildling, Jens Waschke, Detlev Drenckhahn, Peter Hinterdorfer

Journal of Molecular Recognition

AFM Functional Imaging on Vascular Endothelial Cells

Journal:	*Journal of Molecular Recognition*
Manuscript ID:	JMR-09-0125.R1
Wiley - Manuscript type:	Research Article
Date Submitted by the Author:	
Complete List of Authors:	Chtcheglova, Lilia; Institute for Biophysics, University of Linz Wildling, Linda; Institute for Biophysics, University of Linz Waschke, Jens; Institute of Anatomy and Cell Biology, University of Würzburg Drenckhahn, Detlev; Institute of Anatomy and Cell Biology, University of Würzburg Hinterdorfer, Peter; Institute for Biophysics, University of Linz
Keywords:	VE-cadherin, F-actin, AFM, TREC

AFM Functional Imaging on Vascular Endothelial Cells

Lilia A. Chtcheglova,[a]* Linda Wildling[a], Jens Waschke[b], Detlev Drenckhahn[b], and Peter Hinterdorfer[a]

* Correspondence to: L.A. Chtcheglova, Institute for Biophysics, Johannes Kepler University of Linz, A-4040 Linz, Austria.
E-mail: lilia.chtcheglova@jku.at
[a] Institute for Biophysics, Johannes Kepler University of Linz, A-4040 Linz, Austria.
[b] Institute of Anatomy and Cell Biology, University of Würzburg, D-97070 Würzburg Germany.

Keywords: VE-cadherin; F-actin; TREC; AFM

Abstract

Vascular endothelial (VE)-cadherin is predominantly responsible for the mechanical linkage between endothelial cells, where VE-cadherin molecules are clustered and linked through their cytoplasmic domain to the actin-based cytoskeleton. Clustering and linkage of VE-cadherin to actin filaments is a dynamic process and changes according to the functional state of the cells. Here nano-mapping of VE-cadherin was performed using simultaneous topography and recognition imaging (TREC) technique onto microvascular endothelial cells from mouse myocardium (MyEnd). The recognition maps revealed prominent "dark" spots (domains or clusters) with the sizes from 10 to 250 nm. These spots arose from a decrease of oscillation amplitude during specific binding between VE-cadherin *cis*-dimers. They were assigned to characteristic structures of the topography images. After treatment with nocodazole so as to depolymerize microtubules, VE-cadherin domains with a typical ellipsoidal form were still found to be collocalized with cytoskeletal filaments supporting the hypothesis that VE-cadherin is linked to actin filaments. Compared to other conventional techniques such as immunochemistry or single molecule optical microscopy, TREC represents an alternative method to quickly obtain the local distribution of receptors on cell surface with an unprecedented lateral resolution of several nm.

INTRODUCTION

The vascular endothelium forming a first cellular barrier on the inner surface of blood vessels, represents one of the best studied cellular systems where vascular endothelial (VE)-cadherin (7B4/cadherin-5) exerts a relevant role in cell-cell adhesion as well in other important physiological processes such as the control of macromolecular permeability, transmigration of leukocytes, and vascular homeostasis (Dejana, 2008). VE-cadherin belongs to the wide spread und functional important family of calcium-dependent cell adhesion molecules, cadherins, which are single-pass transmembrane glycol-proteins known to be crucial for calcium-dependent, homotypic (or homophilic) cell-cell adhesion (Hyafil, 1981; Takeichi, 1995, Gumbiner, 1996; Patel, 2003)). VE-cadherin is the major adhesion molecule of endothelial adherent junctions and known to be primarily responsible for mechanical linkage between endothelial cells. Recent studies indicate that VE-cadherin-mediated binding is disrupted during TNF-α-induced endothelial barrier breakdown in vivo since a tandem peptide targeting the VE-cadherin adhesive interface blocked the permeability increase in response to TNF-α (Heupel, 2009). It is believed that VE-cadherin molecules are clustered and linked through their cytoplasmic domain to the actin-based cytoskeleton (Figure 1) (Hirano, 1987; Yap 1997; Vincent, 2004). This is supported by the findings that depolymerization of actin filaments reduced VE-cadherin-mediated binding and drastically increased permeability in vivo ((Baumgartner, 2003; Waschke, 2005). Therefore, cytoskeletal anchorage of cadherin is thought to be important for the strengthening of cadherin-mediated adhesion (Yap, 1997; Kemler, 1989; Angst, 2001) mediated by EC domains (Schan, 2000), which enable to associate in parallel lateral *cis*-dimers in physiological Ca^{2+} concentration (~ 1.8 mM) (Shapiro, 1995; Nagar, 1996; Brieher, 1996; Takeda, 1999; Koch 1999; Baumgartner, 2000) (Figure 1 B). The parallel *cis*-dimer is appeared to be the basic structural functional unit to promote a homophilic bond between cells (Shapiro, 1995; Brieher, 1996; Takeda, 1999; Chappuis-Flament, 2001) and these cadherin dimers are assumed to contain one or two binding sites (Shapiro, 1995; Yap, 1998; Takeda, 1999; Koch, 1999;) to form *trans*-interacting antiparallel tetramers or adhesion dimers (Koch, 1999) (Figure 1 C). It was early suggested that by repeating such *trans*-interactions, linear cell-adhesion zipper, which bridge two adjacent cells, can be formed (Shapiro, 1995). However, a quite different picture of two-dimensional molecular organization of cadherins in desmosomes (He, 2003) and on the free cell surface (Iino, 2001; Baumgartner, 2003) has been elucidated. Indeed, individual cadherin molecules have the tendency to form discrete groups (He, 2003) or oligomers (Iino, 2001) or

microdomains (Baumgartner, 2003) and it has been consequently proposed that these preformed cadherin blocks represent the basic building structures for the two-dimensional structures of cell-cell junctions. Moreover, the strength of intercellular adhesion depends on both the surface concentration and adhesive affinity (affinity for *trans*-interaction) of cadherins. The observation that cadherin molecules cluster on the cell surface led to the model that high local concentrations are required for the strong binding between cells. It has been demonstrated that the life time of VE-cadherin trans-interaction is only 550-700 ms which occurs at extremely low affinity (K_D ~ 10^3-10^5 M^{-1} (Baumgartner, 2000a, b), K_D ~ 10^4 M^{-1} (Baumgartner, 2002a)). Such very weak binding properties require the tethering of cadherins to the cytoskeleton in order to guarantee rapid rebinding after dissociation (Baumgartner, 2002b, 2003) Without tethering to the cytoskeleton, cadherins would be driven apart by increased lateral mobility (~10- to 20-fold increase, Baumgartner, 2003) and would require a prolonged time interval for new collision and rebinding. Moreover, such weak binding is partially compensated by a high level of active plasmalemmal VE-cadherin *cis*-dimers on the cell surface (~ 5x10^3 per 1 μm^2 of cell surface (Baumgartner, 2002a)).

Despite this large body of evidence supporting that VE-cadherin molecules are anchored to actin filaments and that anchorage is crucial for adherent junction stability and maintenance of endothelial barrier functions the exact mechanisms underlying this linkage remain to be elucidated. At least in E-cadherin-based adherent junctions a direct anchorage of the cadherin-catenin complex to actin filaments was revealed not to exist (Shapiro and Weiss, 2009). With single molecule fluorescence it was demonstrated that the size of microdomains enriched in actively trans-interacting VE-cadherin was up to ~ 1 μm^2 and these hot spots depended on an intact actin filament system (Baumgartner, 2003). However, due to the limited lateral resolution (from few tens to 200 nm), the recognition sites cannot be resolved on the nm scale nor can they be correlated to topography features. With the recent development of simultaneous topography and recognition imaging (TREC) on model systems (Stroh, 2004a, 2004b; Ebner, 2005) and further progress on cells (Chtcheglova 2007, 2008), it has been illustrated the local distribution of VE-cadherin on vascular endothelial cell surface with unprecedented lateral resolution of 5 nm (Chtcheglova, 2007). Therefore, in the present study we aimed to investigate the local organization of VE-cadherin domains in myocardial microvascular endothelial cells (MyEnd) and to correlate the receptor localization with cell membrane topographical features such as actin filaments.

MATERIALS AND METHODS

Cell culture

A well characterized immortalized microvascular endothelial cell line from mouse myocardium (MyEnd) (Baumgartner, 2003, Adamson 2002) was used. Cells were grown in Dulbecco´s modified Eagles medium (DMEM), supplemented with 50 U/ml penicillin-G, 50 µg streptomycin, and 10% fetal calf serum (FCS) in a humidified atmosphere (5% CO_2) at 37 °C. Cultures were passaged twice a week. For experiments, cells were seeded onto gelatine-coated glass slides (final concentration of gelatine 0.02 %), grown until 70-80 % confluence. To perform AFM measurements, cells were than gently fixed with glutaraldehyde (EM grade 1, Sigma-Aldrich). The solution of glutaraldehyde monomers was added into the medium (final concentration of glutaraldehyde ~ 0.5%) and cells with fixative were subsequently incubated in a humidified atmosphere at 37 °C overnight. Passages 5-20 were used. For pharmacological treatments of MyEnd cortex, stock solutions of nocodazole (4 mg/ml in DMSO) were prepared. The final concentration of nocodazole was ~ 50 µM. Since DMSO can increase the temperature upon mixing with aqueous solutions, first ~ 100 µl of culture medium and mixed with ~ 8 µl of stock drug solution. After reaching room temperature, this solution was added to the Petri dish containing the grown cells and mixed gently with the culture medium (~ 2 ml) to ensure rapid drug delivery to cells. MyEnd cells were than placed at 37 °C for about 80 min and subsequently gently fixed with glutaraldehyde for further AFM measurements.

AFM tip functionalization with VE-cadherin-Fc molecules via PEG-linker

Attachment of a ligand molecule onto the AFM tip converts it into a biospecific molecular sensor to detect a corresponding receptor on a sample surface. Since poly-ethylene glycol (PEG) chains between AFM tips and ligand molecules are particularly advantageous for use in molecular recognition force spectroscopy (MRFS) (Hinterdorfer and Dufrêne, 2006), they are essentially necessary for TREC measurements (Preiner, 2009).

Magnetically coated AFM tips (abbreviated as MAC tips) (Agilent Technologies, Tempe, AZ, USA) were firstly extensively washed in chlorophorm and ethanol, dried with nitrogen and subsequently incubated in ethanolamine-HCl solution (Sigma, 550 mg/ml in dimethylsulfoxide (DMSO)) overnight in order to functionalize the tip surface (Si_3N_4) with amino (-NH_2) groups (Riener, 2003) (Figure 2, step I (a)). Next, PEG chains are attached with

one end to the amino groups on the tip by amide bond formation, for which, PEG linkers possesses an activated carboxy (-COOH) group in the form of an N-hydroxysuccinimide ester (NHS ester) (Figure 2, step II). In the last step, a ligand molecule, a recombinant VE-cadherin (abbreviated as VE-cadherin-Fc), in which the complete extracellular domain of mouse VE-cadherin was fused to the Fc fragment of human IgG (Figure 3) (Baumgartner, 2000a; 2000b) is coupled to the free-tangling end (in this study aldehyde residue) of PEG linker (Bonanni, 2005) (Figure 2, step III).

AFM topographical and dynamic recognition imaging (TREC)

Both AFM topographical and recognition images were acquired in MAC (magnetic alternating current) mode (Han, 1996) using a PicoPlus AFM (Agilent Technologies, Chandler, USA) with magnetically coated tips having a nominal spring constant of 100 pN/nm with a quality factor Q of ~ 1 in liquid. The imaging of living cells was also performed in contact AFM mode. All images were taken in Hank´s balanced salt solution (HBSS) containing 1.8 mM Ca^{2+} at room temperature. The TREC data were obtained by scanning ~ 2x2 μm^2 area of the cell surface with a lateral scan speed of ~ 3.0 µm/sec at 256 or 512 data points per line using a commercially available PicoTREC box (Agilent Technologies, Chandler, USA). In order to block the specific interactions between VE-cadherin-Fc-functionalized tip and MyEnd cell surface, the calcium chelator, 5 mM of ethylenediaminetetraacetic acid (EDTA) was gently injected into the fluid cell of the AFM during scanning.

The operating principle of TREC can be described as following (Figure 4). The functionalized tip with a ligand molecule via a PEG linker is oscillated close to its resonance frequency (~ 10 kHz). The set-point amplitude is adjusted to a value close to the free amplitude. The free amplitude is adjusted to be less that the extended PEG-linker to provide the proper recognition image with high efficiencies and repeatability (Chtcheglova, 2007; Preiner, 2009). When such a tip-tethered ligand binds to its receptor on the sample surface (i.e., when specific molecular recognition occurs), the PEG linker will be stretched during upward movement of the cantilever. The resulting loss in energy will in turn cause the top peaks of the oscillations to be lowered. The ligand-receptor binding events thus become visible due to a reduction in the oscillation amplitude (i.e. recognition signal), as a result of specific recognition during the lateral scan. In contrast to the conventional MAC mode, which exploits a peak-to-peak value of oscillating amplitude (full amplitude) as a feedback parameter, TREC uses the lower part of the oscillation (called as half-amplitude feedback) to

drive a feedback loop for obtaining the topography image, whereas the upper part of the oscillation is used for generation of the recognition image (Figure 4). Moreover, using such sophisticated feedback allows accurate determination of the surface topography (Preiner, 2009). To provide more details, the time-resolved deflection signal of the oscillating cantilever is low-pass filtered to remove the thermal noise, the DC (direct current) is offset levelled and amplified before splitting into the lower (U_{down}) and upper (U_{up}) parts of the oscillations. The signal passes a trigger threshold on each path, and the lower peak of each oscillation period is determined by means of sample and hold analysis. Subsequent peaks form a staircase function, which is then filtered and fed into the AFM controller, where U_{down} drives the feedback loop to record the topography image and U_{up} provides the information to establish the corresponding recognition image. Moreover, the utilization of cantilevers with low Q factor (~ 1 in liquid) in combination with a proper chosen driving frequency and amplitude regime enables the that both types of information are unrelated (Ebner, 2005; Preiner, 2009).

Image processing

Topographical images are represented either by a 512 x 512 or 256 x 256 matrixes. The collected AFM raw data (height image) are used as initial data, which were subsequently imported and analyzed into MATLAB Version 7 (MathWorks Inc., Natick, NA). The further line-wise flattening, plane fitting and contrast enhancement have been performed as in (Kienberger, 2006). All programs employed in this work can be found on MATLAB file-exchange.

RESULTS AND DISCUSSION

Morphology of MyEnd cells

MyEnd cells grown to subconfluent monolayers and the corresponding AFM topography images (Figure 5) illustrate a characteristic morphology that was previously obtained with light microscope (Baumgartner, 2003). These cells are organized into whirl-like formations, they are highly elongated (~ 80 or even more µm in length, with tens of µm in diameter), and the cell heights vary from ~ 100 nm at the periphery to ~ 1-2 µm on the nucleus (Figure 5 A, B).

In order to overcome the circumstances for the recognition imaging such as the cell elasticity and the lateral diffusion of receptors (e.g. of VE-cadherin (Baumgartner, 2003)), a

fixation procedure as for immunochemistry experiences can be applied. In our studies, the cells were fixed with glutaraldehyde. The fixation procedure makes the soft biological objects stiffer and as a consequence, it generally gives access to high lateral resolution in AFM images as it was observed with proteins (GroES) (Mou, 1996). However, the common fixation of cells in buffer solution at room temperature causes the smoothing of the cell surface with the loss of most filamentous features, which were seen in AFM pictures of living cells (Figure 5 A) (Pesen and Hoh, 2005) as well nucleus become visible presumably due to the membrane collapse during dehydration caused by the fixation procedure. When the unpurified solution of glutaraldehyde is used the undesirable formation of globular large features on the cell surface (e.g. polymers of glutaraldehyde) can be detected as well. We found a method to gently fix the cells with the solution of glutaraldehyde containing monomers (EM grade) similar to the procedure described by (Oberleithner, 2003). The prepared stock solution of glutaraldehyde (~ 200 µL, 5% in HBSS) was added and gently mixed with the culture medium (~ 2 ml), the cells were then incubated at 37 ° C as cultured before (for more details see Materials and Methods section). Such method is likely prevent unexpected osmotic and temperature changes in the cell culture medium. As a result, the cell volume as well the filamentous structures of cytoskeleton are mostly preserved (Figure 5 B) that makes possible further AFM investigations at a subcellular level. Figure 5 D, E represent typical AFM images of gently fixed MyEnd cell membrane at high magnification of ~ 5x5 μm^2. The complex filamentous networks with wide range of forms can be usually observed. Following treatment with nocodazole to depolymerize microtubules the filamentous structure of the cell cortex was conserved (Figure 5 E).

Nano-mapping of VE-cadherins on gently fixed MyEnd cell surface treated with nocodazole

Since VE-cadherin is cell specific and firmly located at intercellular junctions (Lampugnani, 1997; Baumgartner, 2003), TREC images were collected on the contact region between adjacent cells with VE-cadherin-Fc-functionalized tip in calcium reach buffer solution (i.e. HBSS containing 1.8 mM Ca^{2+}). As previously observed the topography of a scanned cell surface area (Figure 6 A) demonstrates a complex picture of linear and branched filaments with some globular features. In addition, the enlarged number of filaments with a typical width of ~ 60-70 nm is clearly visible (Figure 6 A).The local roughness was estimated as ~ 24 nm and the lateral resolution as ~ 5 nm. In our first TREC studies on MyEnd cells (Chtcheglova, 2007) we observed, that VE-cadherin forms microdomains with dimensions

from ~ 10 to ~ 100 nm, which were nonuniformly distributed on the cellular surface. Interestingly, only a few domains (~ 4 from ~ 56 detected) were found directly on the top of filaments and most spots were located near and between filaments, thus indicating the incomplete clustering of VE-cadherin molecules. In this study the corresponding simultaneously recorded recognition maps contain again "dark" spots (Figure 6 B) (amplitude reduction up to 2 nm) with inhomogeneous distribution. These dark spots reflect the microdomains typically with ellipsoidal form (Figure 7 A) and dimensions from ~10 to ~250 nm, with a mean ± SD of 162±55 nm (n=56) for the long axis (Figure 7 B). A closer look at the recognition spots (Figure 7 A) reveals their characteristic ellipsoidal form and that they consist of one large domain with typical sizes of ~ 80 nm (Figure 7 B) or ~ 180 nm surrounded by few smaller domains (10–20 nm). With comparison to the results observed on the early confluent MyEnd cells (Chtcheglova, 2007), the number of single events was significantly decreased. The spots with dimensions of ~ 8-16 nm were identified as single *cis*-dimers taking into account the size of the VE-cadherin *cis*-dimer (diameter ~ 3 nm) and the free orientation of PEG-linker leading to the specific binding even before/after the binding site position. Nevertheless, the drastical increase in the spot sizes accompanying by practical disappearance of small domains (Figure 7 B) and consequent rise in the number of active *cis*-dimers (more than 6000/μm^2) imply the complete clustering of VE-cadherin.

The specificity of VE-cadherin recognition process has been verified by addition of calcium chelator, 5 mM EDTA, in the liquid flow cell in which the sample was imaged. Indeed, in the absence of Ca^{2+} functional VE-cadherin *cis*-dimers on the tip dissociate into inactive monomers (Baumgartner, 2000) (Figure 2 B) that leads to the blocking of specific VE-cadherin *trans*-binding. This effect results in the disappearance of almost all binding events in the recognition image (Figure 6 B'), whereas no change in the topography image has been observed (Figure 6 B). The resolution of the recognition technique is generally limited by the linker length (here to ~ 8 nm).

The receptor binding sites can properly be assigned to the topographical features for heterogeneous biological surfaces such as cells or membrane fragments. Figure 8 illustrates the superimposition of the recognition map (Figure 6 A') onto the corresponding topographical image (Figure 6 A). This procedure allows revealing the locations of receptors in the topographical image with high lateral resolution and high efficiency. Repeated measurements indicate that the size of VE-cadherin domains ranges from 10 to as much as 250 nm. In addition, these domains can be easily aligned to the filaments seen in topography image (Figure 8). These observations directly illustrate the clustering of VE-cadherin *cis*-

dimers on cell surface and as well support the hypothesis of VE-cadherin anchorage to the F-actin cytoskeleton.

CONCLUSION

It has been previously reported the potential use of AFM in order to localize and identify of membrane receptors (Eppell, 1995) and ion channels (Smith, 1997). However, these studies have to rely on the use of immunogold particles or fluorescent labeling that needs a combination of AFM with fluorescence microscopy. Such an approach makes it easier AFM topography imaging, however it certainly limits the imaging resolution to molecular scales (e.g. particle or fluorescent label size) at best. Here and previously (Chtcheglova, 2007) we demonstrated the applicability of AFM based TREC technique to gently fixed endothelial cells to visualize VE-cadherin binding sites by using VE-cadherin-Fc – functionalized AFM tips. The recognition map of VE-cadherins contained "dark" spots due to decrease of oscillation amplitude of AFM tip during specific binding between VE-cadherin *cis*-dimers. In the present study, VE-cadherins were again not uniformly distributed but located mostly along the F-actin filaments, and organized in microdomains or clusters with dimensions from 10 to 250 nm, which were at least four times smaller that observed by using single molecule optical microscopy (Baumgartner, 2003). The effect that most VE-cadherin domains were found on the top of filaments (Figure 8) clear demonstrates the anchorage of VE-cadherin to the F-actin filaments. The typical sizes (~ 100 and 180 nm) (Figure 6 B) and ellipsoidal shapes (Figure 7, 8) of spots indicate the complete clustering of VE-cadherin. The specific Ca^{2+} dependent VE-cadherin *trans*-interaction was abolished by addition of EDTA that lead to the disappearance of specific domains in recognition images.

In addition, TREC technique offers the advantage that structural information (e.g. topography) and recognition maps can be recorded simultaneously at the same speed as that used for the conventional topographic imaging, typically several minutes per image. Another major improvement of TREC over conventional fluorescence approaches to cells is the spatial and recognition resolution obtained in the present work of ~ 5 and ~ 8 nm, respectively. Therefore, the exploitation of dynamic recognition imaging allows to detect single molecular interactions, and thus visualize, identify, and quantify local receptor binding sites and to assign their locations to the topographical features of the cell surface with several nm accuracy. We strongly believe that the described here TREC methodology can be successfully

used for many adherent cells or extracted cellular membranes in order to identify locally different receptor binding sites.

PERSPECTIVES

The TREC approach to live cell investigations represents certainly a more challenging task. Some TREC images collected on live vascular endothelial cells with antibody-coated tip have been recently reported (Van Vliet and Hinterdorfer, 2006). However, in these studies the experimental conditions such as the specificity, efficiency and repeatability of recognition were not described in details. It is important to note several current limitations of this contact-based approach such as scanning rate. For instance, the rates of lateral diffusion and internalization of receptors within the cell membrane should be considered with respect to experimentally attainable scanning rates and resolutions. The potential to induce confusing cell responses by mechanical perturbing of the cell surface and its receptors during scanning should be also recognized. Nevertheless, by taking account these constrains with further improvements of AFM (e.g. resolution and acquisition time) we expect that this dynamic mapping of ligand-receptor interactions at the single cell level will be valid to living cells.

Acknowledgements

This work was supported by European Community (EC) project “Bio-Light-Touch” (FP6-2004-NEST-C-1-028781).

REFERENCES

Adamson RH, Curry FE, Adamson G, Liu B, Jiang Y, Aktories K, Barth H, Daigeler A, Golenhofen N, Ness W, Drenckhahn D. 2002. Rho and rho kinase modulation of barrier properties: cultured endothelial cells and intact microvessels of rats and mice. J. Physiol. 539: 295-308.

Angst BD, Marcozzi C, Magee AI. 2001. The cadherin super-family: diversity in form and function. J. Cell Sci. 114: 629-641.

Baumgarther W, Hinterdorfer P, Ness W, Raab A, Vestweber D, Schindler H, Drenckhahn D. 2000a. Cadherin interaction probed by atomic force microscopy. Proc. Natl. Acad. Sci. USA. 97: 4005-4010.

Baumgartner W, Gruber HJ, Hinterdorfer P, Drenckhahn D. 2000b. Affinity of trans-interacting VE-cadherin determined by atomic force microscopy. Single Mol. 2: 119-122.

Baumgartner W, Drenckhahn D. 2002a. Plasmalemmal concentration and affinity of mouse vascular endothelial cadherin, VE-cadherin. Eur. Biophys. J. 31: 532-538.

Baumgartner W, Drenckhahn D. 2002b. Transmembrane cooperative linkage in cellular adhesion. Eur. J. Cell Biol. 81: 161-168.

Baumgartner W, Schütz GJ, Wiegand J, Golenhofen N, Drenckhahn D. 2003. Cadherin function probed by laser tweezer and single molecule fluorescence in vascular endothelial cells. J. Cell Sci. 116: 1001-1011.

Bonanni B, Kamruzzahan ASM, Bizzarri AR, Rankl C, Gruber HJ, Hinterdorfer P, Cannistraro S. 2005. Single molecule recognition between cytochrome C 551 and gold-immobilized azurin by force spectroscopy. Biophys. J. 89: 2783-2791.

Brieher WM, Yap AS, Gumbiner BM. 1996. Lateral dimerization is required for the homophilic binding activity of C-cadherin. J. Cell Biol. 135: 487-496.

Chappuis-Flament S, Wong E, Hicks LD, Kay CM, Gumbiner BM. 2001. Multiple cadherin extracellular repeats mediate homophilic binding and adhesion. J. Cell Biol. 154: 231-243.

Chtcheglova LA, Waschke J, Wildling L, Drenckhahn D, Hinterdorfer P. 2007. Nano-scale dynamic recognition imaging on vascular endothelial cells. Biophys. J. 93: L11-L13.

Chtcheglova LA, Atalar F, Ozbek U, Wildling L, Ebner A, Hinterdorfer P. 2008. Localization of ergtoxin-1 receptors on the voltage sensing domain of hERG K^+ channel by AFM recognition imaging. Pflugers Arch. Eur. J. Physiol. 456: 247-254.

Dejana E, Orsenigo F, Lampugnani MG. 2008. The role of adherents junctions and VE-cadherin in the control of vascular permeability. J. Cell. Sci. 121: 2115-2122.

Ebner A, Kienberger F, Kada G, Stroh CM, Geretschläger M, Kamruzzahan ASM, Wildling L, Johnson WT, Ashcroft B, Nelson J, Lindsay SM, Gruber HJ, Hinterdorfer P. 2005. Localization of single avidin-biotin interactions using simultaneous topography and molecular recognition imaging. ChemPhysChem. 6: 897-900.

Eppell SJ, Simmons SR, Albrecht RM, Marchant RE. 1995. Cell-surface receptors and proteins on platelet membranes imaged by scanning force microscopy using immunogold contrast enhancement. Biophys. J. 68: 671-680.

Gumbiner BM. 1996. Cell adhesion: the molecular basis of tissue architecture and morphogenesis. Cell. 84:345-357.

Han W, Lindsay SM, Jing T. (1996). A magnetically driven oscillating probe microscope for operation in liquids. Appl. Phys. Lett. 69: 4111-4113.

He W, Cowin P, Stokes DL. 2003. Untagling desmosomal knots with electron tomography. Science. 302: 109-113.

Heupel W-M, Efthymiadis A, Schlegel N, Müller Th, Baumer Y, Baumgartner W, Drenckhahn D, Waschke J. 2009. Endothelial barrier stabilization by a cyclic tandem peptide targeting VE-cadherin transinteraction in vitro and in vivo. J. Cell Sci. 122: 1616-1625.

Hinterdorfer P, Dufrêne YF. 2006. Detection and localization of single molecular recognition events using atomic force microscopy. Nat. Methods 3: 347-355.

Hirano S, Nose A, Hatta K, Kawakami A, Takeichi M. 1987. Calcium-dependent cell-cell adhesion molecules (cadherins): subclass specificities and possible involvement of actin bundles. J. Cell Biol. 105: 2501-2510.

Hyafil F, Babinet C, Jacob F. 1981. Cell-cell interactions in early embryogenesis: a molecular approach to the role of calcium. Cell. 26: 447-454.

Iino R, Koyama I, Kusumi A. 2001. Single molecule imaging of green fluorescent proteins in living cells: E-cadherin forms oligomers on the free cell surface. Biophys. J. 80: 2667-2677.

Kemler R, Ozawa M. 1989. Uvomorulin-catenin complex: cytoplasmic anchorage of a Ca^{2+} -dependent cell adhesion molecule. Bioessays. 11: 88-91.

Kienberger F, Pastushenko VP, Kada G, Puntheeranurak T, Chtcheglova L, Riethmueller C, Rankl C, Ebner A, Hinterdorfer P. 2006. Improving the contrast of topographical AFM images by a simple averaging filter. Ultramicroscopy. 106: 822-828.

Koch AW, Bozic D, Pertz O, Engel J. 1999. Homophilic adhesion by cadherins. Curr. Opin. Struct. Biol. 9: 275-281.

Lampugnani MG and Dejana E. 1997. Interendothelial junctions: structure, signaling and functional roles. Curr. Opin. Cell Biol. 9: 674-682.

Mou J, Czajkowsky DM, Sheng SJ, Ho R, Shao Z. 1996. High resolution surface structure of E. coli GroES oligomer by atomic force microscopy. FEBS Lett. 381: 161-164.

Nagar B, Overduin M, Ikura M, Rini JM. 1996. Structural basis of calcium-induced E-cadherin rigidification and dimerization. Nature. 380: 360-364.

Oberleithner H, Schneider SW, Albermann L, Hillebrand U, Ludwig T, Riethmüller C, Shahin V, Schäfer C, Schillers H. 2003. Endothelial cell swelling by aldosterone. J. Membrane Biol. 196: 163-172.

Patel SD, Chen CP, Bahna F, Honig B, Shapiro L. 2003. Cadherin-mediated cell-cell adhesion: sticking together as a family. Curr. Opin. Struct. Biol. 13: 690-698.

Pesen D, Hoh JH. 2005. Micromechanical architecture of the endothelial cell cortex. Biophys. J. 88: 670-679.

Preiner J, Ebner A, Chtcheglova L, Zhu R, Hinterdorfer P. 2009. Simultaneous topography and recognition imaging: physical aspects and optimal imaging conditions. Nanotechnology 20: 215103-215121.

Riener CK, Stroh CM, Ebner A, Klampfl C, Gall AA, Romanin C, Lyubchenko YL, Hinterdorfer P, Gruber HJ. 2003. Simple test for single molecule recognition force microscopy. Anal. Chim. Acta. 479: 59-75.

Shan W-S, Tanaka H, Philips GR, Arndt K, Yoshida M, Colman DR, Shapiro L. 2000. Functional cis-heterodimers of N- and R-Cadherins. J. Cell Biol. 148: 579-590.

Shapiro L, Fannon AM, Kwong PD, Thompson A, Lehmann MS, Grübel G, Legrand J-F, Als-Nielsen J, Colman DR, Hendrickson WA. 1995. Structural basis of cell-cell adhesion by cadherins. Nature. 374: 327-337.

Shapiro L, Weis WI. 2009. Structure and biochemistry of cadherins and catenins. Cold Spring Harb. Perspect. in Biol 1: a003053.

Smith PR, Bradford AL, Schneider S, Benos DJ, Geibel JP. 1997. Localization of amiloride-sensitive sodium channels in A6 cells by atomic force microscopy. Am. J. Physiol. Cell Physiol. 272: C1295-C1298.

Stroh CM, Ebner A, Geretschläger M, Freudenthaler G, Kienberger F, Kamruzzahan ASM, Smith-Gill SJ, Gruber HJ, Hinterdorfer P. 2004a. Simultaneous topography and recognition imaging using force microscopy. Biophys. J. 87: 1981-1990.

Stroh C, Wang H, Bash R, Ashcroft B, Nelson J, Gruber H, Lohr D, Lindsay SM, Hinterdorfer P. 2004b. Single-molecule recognition imaging microscopy. Proc Natl Acad Sci USA. 101: 12503-12507.

Takeda H, Shimoyama Y, Nagafuchi A, Hirohashi S. 1999. E-cadherin functions as a cis-dimer at the cell-cell adhesive interface in vivo. Nat. Struct. Biol. 6: 310-312.

Takeichi M. 1995. Morphogenetic roles of classical cadherins. Curr. Opin. Cell Biol. 7: 619-627.

Van Vliet KJ, Hinterdorfer P. 2006. Probing drug-cell interactions. Nanotoday. 1: 2-9.

Vincent PA, Xiao K, Buckley KM, Kowalczyk AP. 2004. VE-cadherin: adhesion at arm's length. Am. J. Physiol. Cell Physiol. 286: C987-C997.

Waschke J, Curry FE, Adamson RH, Drenckhahn D. 2005. Regulation of actin dynamics is critical for endothelial barrier functions. Am. J. Physiol. Heart Circ. Physiol. 288: H1296-H1305.

Yap AS, Brieher WM, Gumbiner BM. 1997. Molecular and functional analysis of cadherin-based adherent junctions. Annu. Rev. Cell. Dev. Biol. 13: 119-146.

Yap AS, Niessen CM, Gumbiner BM. 1998. The juxtamembrane region of the cadherin cytoplasmic tail supports lateral clustering, adhesive strengthening, and interaction with $p120^{ctn}$. J. Cell Biol. 141: 779-789.

Figure Legends

Figure 1. A) Scheme of VE-cadherin domain organization. As other cadherins VE-cadherin is characterized by the presence of 5 sequence repeats of ~ 110 amino acids, which form folded Greek-key topology extracellular (EC) domains. The connections between successive domains are rigidified by conserved Ca^{2+}-binding sites representing the most significant feature of the repeat sequences. The cytoplasmic domain of VE-cadherin includes the "juxtamembrane region" that binds p120-catenin ($p120^{ctn}$) and the "catenin binding domain" that interacts with β-catenin and plakoglobin. B) In the presence of extracellular Calcium (1.8 mM) the rigid cadherin extracellular domains (shown as grey rods) enable to associate in functional *cis*-dimers. The calcium binding sites between extracellular domains are shown as stars. C) These active cadherin *cis*-dimers promote a homophilic bond between adjacent cells by forming a *trans*-adhesion dimer.

Figure 2. Coupling scheme for tethering proteins to AFM tips by using aldehyde-PEG-NHS linker. I) The aminofunctionalization of silicon nitride tips can be performed either with ethanolamine-hydrochloride (a, present work) or in gas phase with 3-minopropyltriethoxysilane (APTES) (b). II) After aminofunctionalization a poly(ethelene glycol) (PEG) chain is attached via its amino-reactive terminus (e.g. NHS-ester). III) The aldehyde residues on the free end can be further conjugated to the amino groups of the lysine residues of the protein. Reaction of protein and aldehyde results in the formation of Schiff base, which is subsequently fixed by reduction with $NaCNBH_3$.

Figure 3. Active (A) and inactive (B) forms of recombinant VE-cadherin *cis*-dimer, which was attached to the AFM tip via PEG-linker and scanned over MyEnd cell surface (C).

Figure 4. Schematic of TREC functioning. The raw cantilever deflection signal is fed into the TREC box, where the maxima (U_{up}) and the minima (U_{down}) of each oscillation period are used for the recognition and the topography image, respectively.

Figure 5. AFM topography images of MyEnd cells obtained either with contact mode (A) or MAC mode (B-E). A) Living cells. B, D) Gently fixed cells and C, E) cells treated with nocodazole and subsequently gently fixed with glutaraldehyde. Cells were grown either in early subconfluent state (images were taken after 1-2 days after seeding) (A, B and D) or in

mature subconfluent state (C, E) (after 3-4 days after seading). Color scale (dark grey to white) for A-C is 0 - 1.5 μm and for D, E 0 – 60 nm, respectively.

Figure 6. Simultaneously topography (A) and recognition images (A') recorded on MyEnd cell surface (2x2 μm^2) treated with 50 μM of nocodazole for 80 min and subsequently gently fixed with glutaraldehyde. The reduction of oscillating amplitude was used as recognition signal. The recognition efficiency was generally high and remains so on several subsequent rescans. After addition of 5 mM EDTA in the fluid cell the recognition spots (dark red domains) disappeared (B') as the active VE-cadherin-Fc *cis*-dimers on the AFM tip dissociated in inactive monomers, thus abolishing specific VE-cadherin *trans*-interaction. Blocking experiments did not affect the membrane topography (B).

Figure 7. A) Example of a typical VE-cadherin domain with ellipsoidal form (a≈65 nm; b≈140 nm) embedded by several (4-5) spots with smaller size of 5 – 40 nm. The domain was magnified from the corresponding recognition map (Figure 6 A'). Recognition domains were depicted by threshold analysis (threshold = - 1.7 nm) and bordered by white lines. B) Distribution of VE-cadherin size spots obtained on cell surface treated with nocodazole.

Figure 8. Locations of VE-cadherin domains (in green) on the MyEnd cellular surface treated with nocodazole (topographical image from Figure 6 A). It is clear seen, that the most domains are detected on the actin filaments.

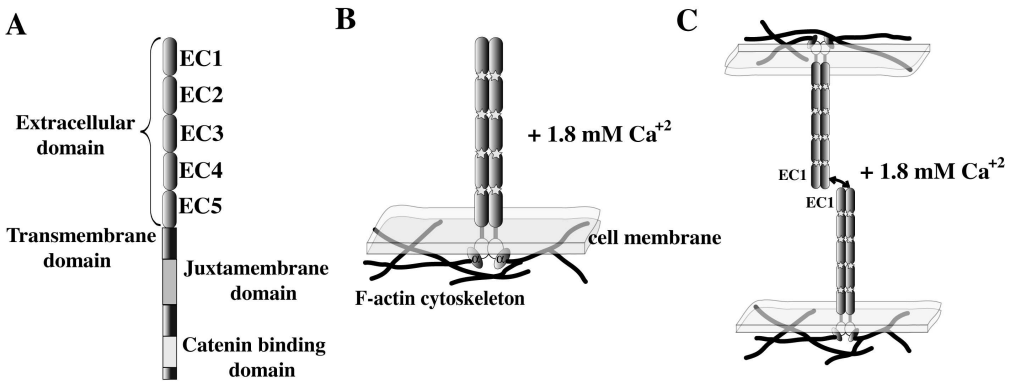

Figure 1. A) Scheme of VE-cadherin domain organization. As other cadherins VE-cadherin is characterized by the presence of 5 sequence repeats of ~ 110 amino acids, which form folded Greek-key topology extracellular (EC) domains. The connections between successive domains are rigidified by conserved Ca2+-binding sites representing the most significant feature of the repeat sequences. The cytoplasmic domain of VE-cadherin includes the "juxtamembrane region" that binds p120-catenin (p120ctn) and the "catenin binding domain" that interacts with β-catenin and plakoglobin. B) In the presence of extracellular Calcium (1.8 mM) the rigid cadherin extracellular domains (shown as grey rods) enable to associate in functional cis-dimers. The calcium binding sites between extracellular domains are shown as stars. C) These active cadherin cis-dimers promote a homophilic bond between adjacent cells by forming a trans-adhesion dimer.
238x92mm (300 x 300 DPI)

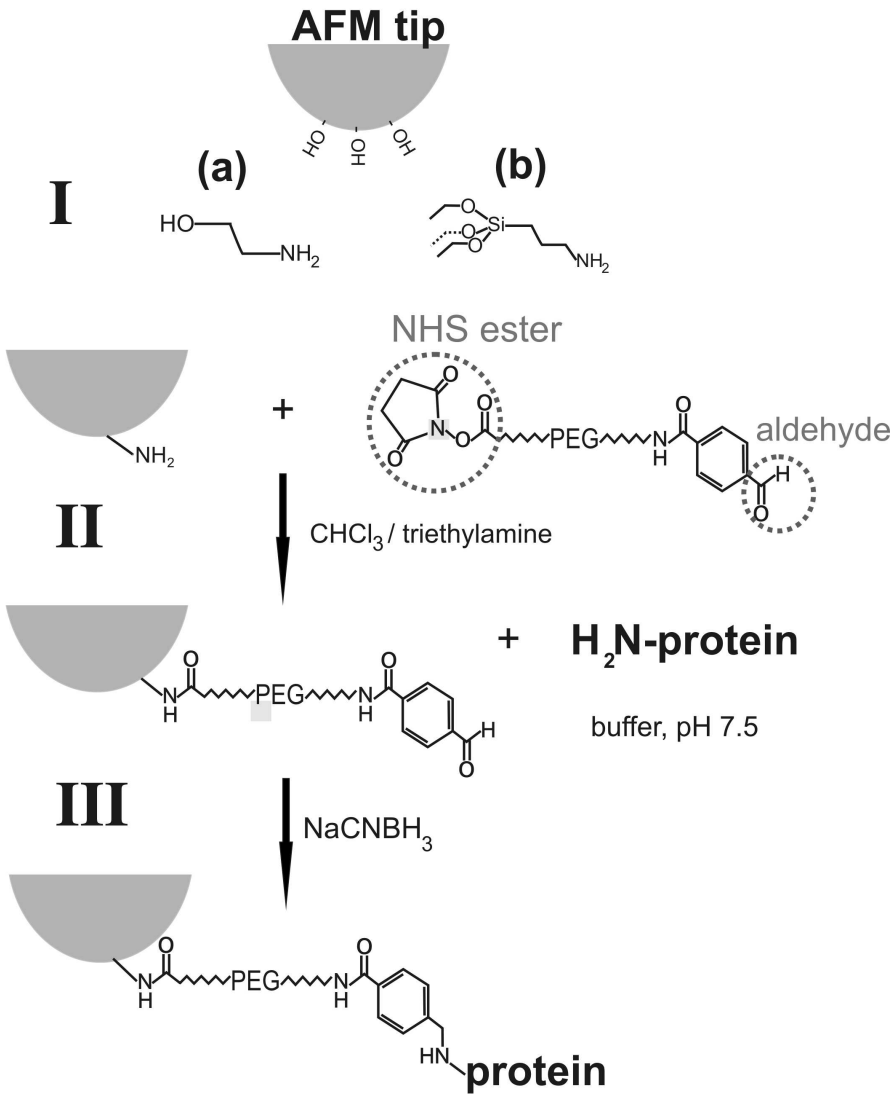

Figure 2. Coupling scheme for tethering proteins to AFM tips by using aldehyde-PEG-NHS linker. I) The aminofunctionalization of silicon nitride tips can be performed either with ethanolamine-hydrochloride (a, present work) or in gas phase with 3-minopropyltriethoxysilane (APTES) (b). II) After aminofunctionalization a poly(ethelene glycol) (PEG) chain is attached via its amino-reactive terminus (e.g. NHS-ester). III) The aldehyde residues on the free end can be further conjugated to the amino groups of the lysine residues of the protein. Reaction of protein and aldehyde results in the formation of Schiff base, which is subsequently fixed by reduction with NaCNBH3.
184x241mm (300 x 300 DPI)

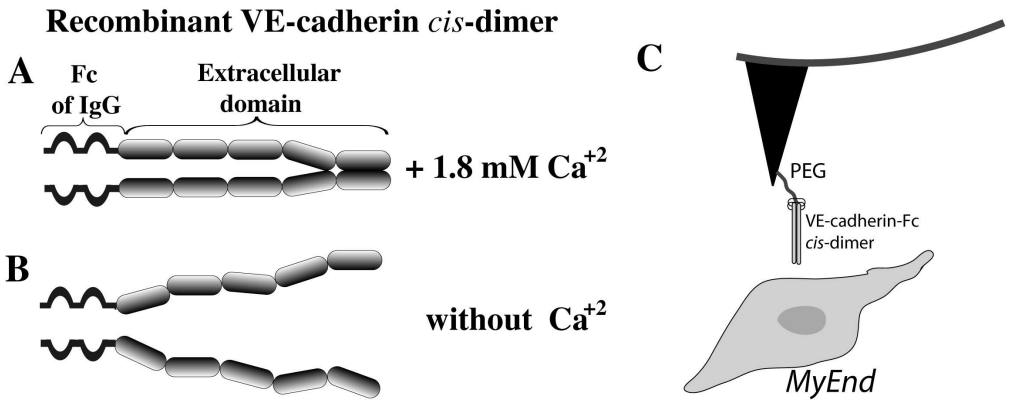

Figure 3. Active (A) and inactive (B) forms of recombinant VE-cadherin cis-dimer, which was attached to the AFM tip via PEG-linker and scanned over MyEnd cell surface (C).
194x77mm (300 x 300 DPI)

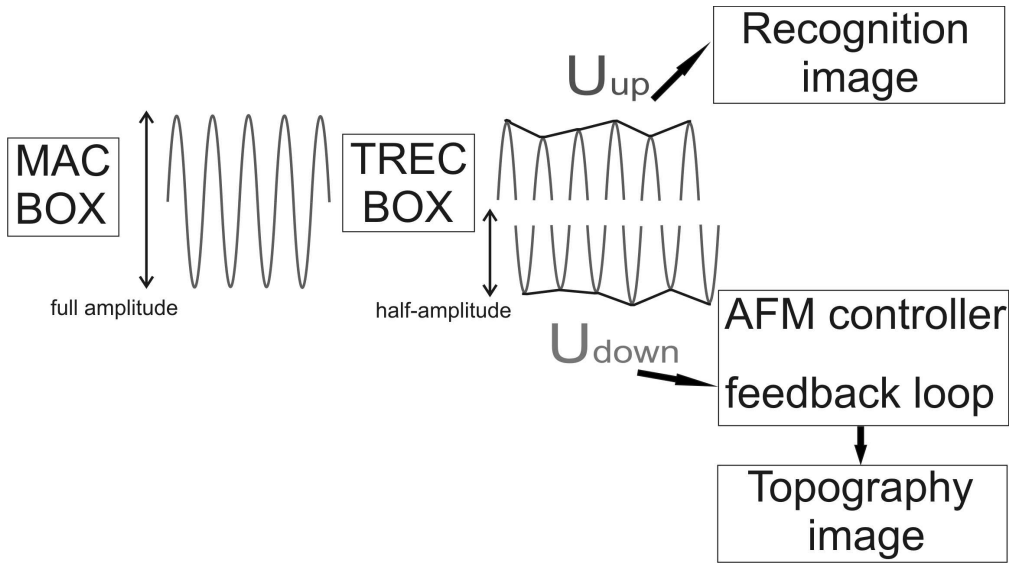

Figure 4. Schematic of TREC functioning. The raw cantilever deflection signal is fed into the TREC box, where the maxima (Uup) and the minima (Udown) of each oscillation period are used for the recognition and the topography image, respectively.
195x108mm (300 x 300 DPI)

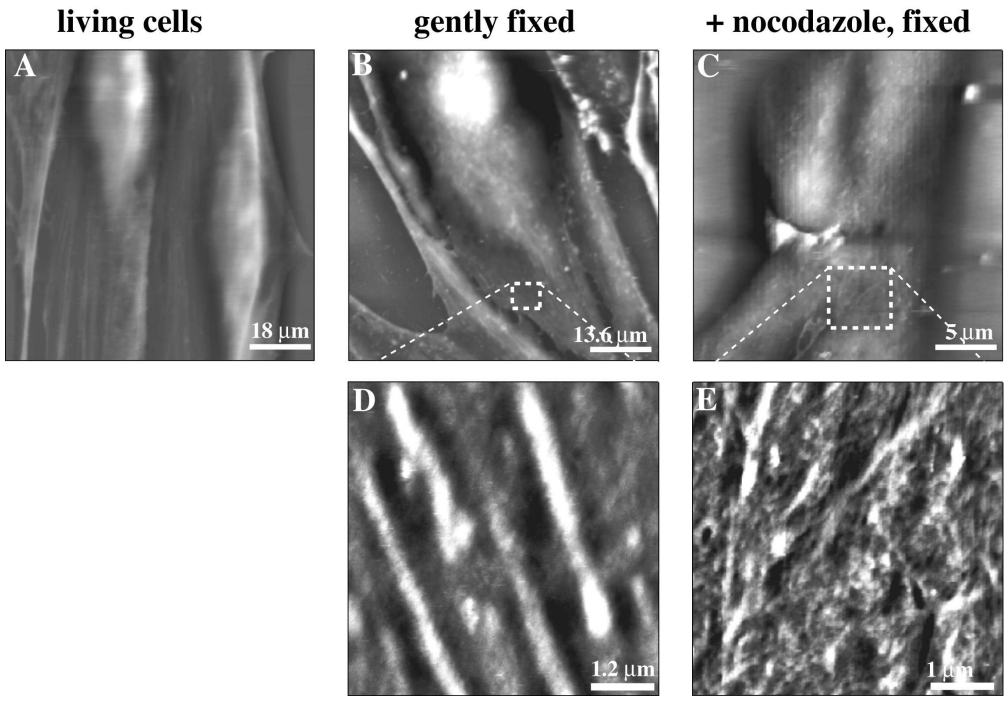

Figure 5. AFM topography images of MyEnd cells obtained either with contact mode (A) or MAC mode (B-E). A) Living cells. B, D) Gently fixed cells and C, E) cells treated with nocodazole and subsequently gently fixed with glutaraldehyde. Cells were grown either in early subconfluent state (images were taken after 1-2 days after seeding) (A, B and D) or in mature subconfluent state (C, E) (after 3-4 days after seading). Color scale (dark grey to white) for A-C is 0 - 1.5 µm and for D, E 0 – 60 nm, respectively.
193x134mm (300 x 300 DPI)

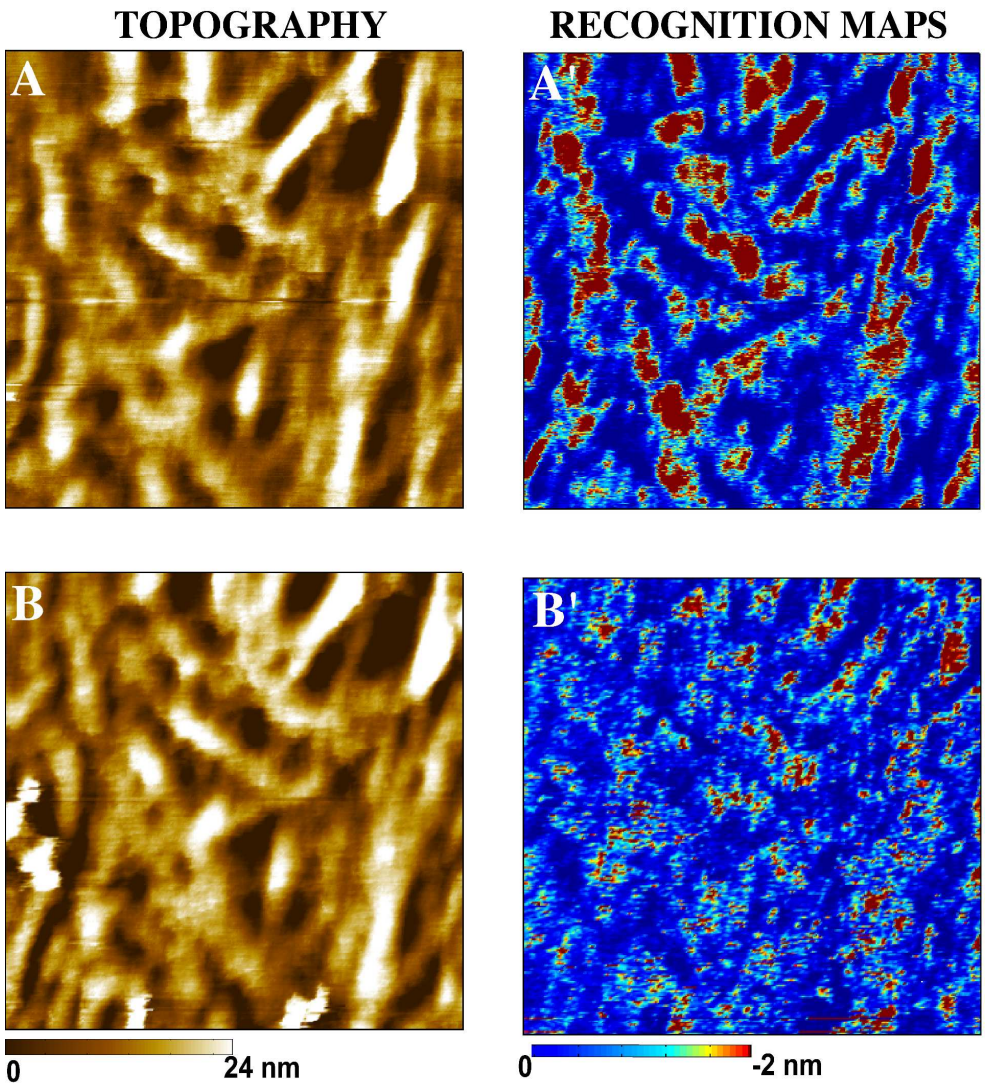

Figure 6. Simultaneously topography (A) and recognition images (A') recorded on MyEnd cell surface (2x2 μm2) treated with 50 μM of nocodazole for 80 min and subsequently gently fixed with glutaraldehyde. The reduction of oscillating amplitude was used as recognition signal. The recognition efficiency was generally high and remains so on several subsequent rescans. After addition of 5 mM EDTA in the fluid cell the recognition spots (dark red domains) disappeared (B') as the active VE-cadherin-Fc cis-dimers on the AFM tip dissociated in inactive monomers, thus abolishing specific VE-cadherin trans-interaction. Blocking experiments did not affect the membrane topography (B).
165x180mm (600 x 600 DPI)

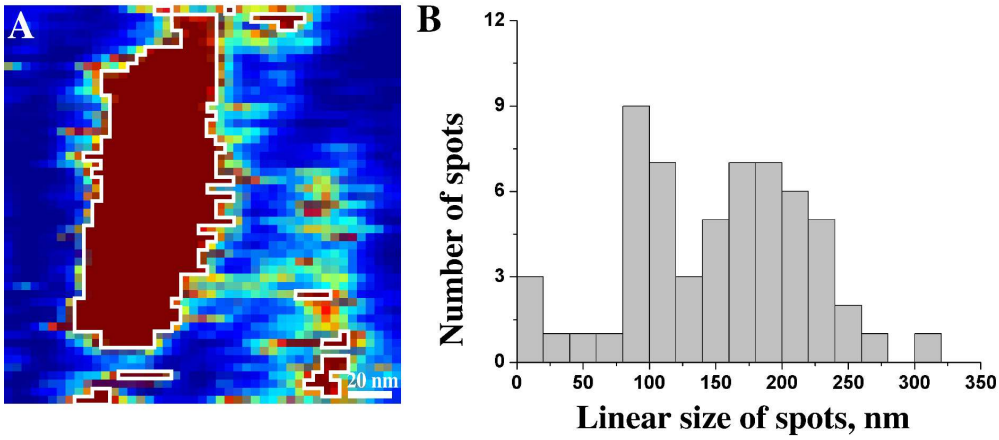

Figure 7. A) Example of a typical VE-cadherin domain with ellipsoidal form (a≈65 nm; b≈140 nm) embedded by several (4-5) spots with smaller size of 5 – 40 nm. The domain was magnified from the corresponding recognition map (Figure 6 A'). Recognition domains were depicted by threshold analysis (threshold = - 1.7 nm) and bordered by white lines. B) Distribution of VE-cadherin size spots obtained on cell surface treated with nocodazole.
191x85mm (500 x 500 DPI)

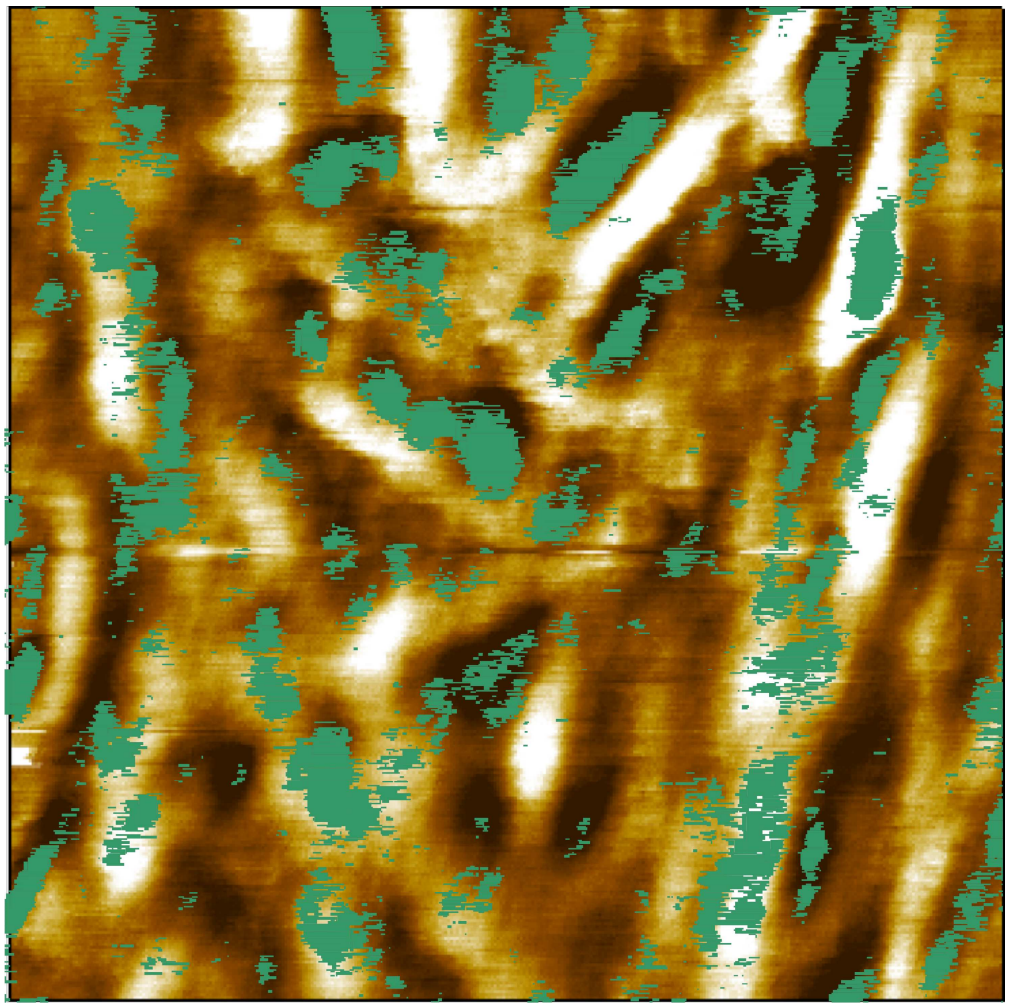

Figure 8. Locations of VE-cadherin domains (in green) on the MyEnd cellular surface treated with nocodazole (topographical image from Figure 6 A). It is clear seen, that the most domains are detected on the actin filaments.
124x124mm (600 x 600 DPI)